Journal of Advanced Manufacturing Science and Technology 5(4) (2025) 2025024

Journal of
Advanced Manufacturing Science and Technology
jamst@jamstjournal.com;jamst2020@126.com
www.jamstjournal.com

Optimization of process parameters of laser jet sold bonding through response surface ball

Guangzi WANG[a], Mingyue XIONG[a], Zhenghu ZHU[a,b], Cheng YANG[b], Ning QIAN[a,*], Jiuhua XU[a]

[a]*College of Mechanical & Electrical Engineering, Nanjing University of Aeronautics and Astronautics, Nanjing 210016, China*
[b]*Nanjing Institute of Electronic Equipment, Nanjing 210013, China*

Received 25 October 2024; revised 21 November 2024; accepted 30 December 2024; Available online 18 January 2024

Abstract: As electronic packaging technology strives for miniaturization, integration, and multifunctionality, System in Package (SiP) technology faces new challenges. This study delves into Laser Jet Soldering Ball Bonding (LJSBB) technology as an alternative to traditional ball bonding techniques to reduce costs and enhance reliability. Using the method of controlling variables, the study systematically analyzed the impact of three key process parameters: laser power, heating time, and nozzle height, on the morphology of solder joints, coplanarity, and shear strength, revealing their mechanisms of influence. The experimental results indicate that increasing laser power and extending heating time can raise the temperature of the solder ball melt pool, causing the solder joints to flatten, directly affecting coplanarity; increasing nozzle height can make the solder ball move more violently upon contact with the pad, affecting its solidified shape and thus coplanarity. Additionally, it transforms the intermetallic compound (IMC) layer from a dispersed discontinuous state to a continuous thin layer, significantly enhancing the shear strength of the solder joints. Furthermore, through response surface experiments, the study analyzed the interactions between various process parameters. It verified the optimization results of the response surface, which were found to have a minimal error compared to actual values.

Keywords: Electronic packaging; Laser jet solder ball bonding; Coplanarity; Shearing force; Intermetallic compound; Response surface; Process optimization

1. Introduction

System in a Package (SiP) represents an advanced electronic packaging technology, engineered to cater to the demands of miniaturization, heightened integration, and the multifunctional capabilities of electronic devices. It embodies a sophisticated internal structure and intricate process technology. Nonetheless, the multiple heating cycles inherent in the packaging process are bound to exert certain impacts on the device's performance and reliability [1-2]. To mitigate the thermal effects associated with solder ball placement in SiP devices and to enhance the reliability of solder joints, there is an urgent need for innovative technology to supersede conventional approaches. In response, the Laser Jet Solder Ball Bonding (LJSBB) technology has been developed. LJSBB offers several advantages over traditional methods: it operates without the need for high temperature and high-pressure conditions, it reduces soldering time, and it eliminates the necessity for flux. The resulting interfaces are of superior quality, with intermetallic compounds that are more uniform and thinner. Additionally, LJSBB is associated with a lower void rate, improved mechanical properties, greater shearing force, and slower aging processes [3]. Moreover, LJSBB is advantageous for repair operations, as it exerts less impact on high-density solder joints and maintains a lower peak temperature compared to traditional methods. This results in a reduced impact of repair heat on the overall device reliability [4]. Beyond its role as a replacement for traditional techniques, Fettke et al. [5] has also successfully employed LJSBB to implement the VIA structure in solder ball stacking, demonstrating superior performance across all evaluated aspects compared to traditional ball stacking technologies.

The Laser Jet Solder Ball Bonding process [6], as depicted in Fig. 1, involves the irradiation of a laser beam that melts the solder ball into a liquid state. Upon reaching the predetermined heating time, nitrogen will propel the molten ball through the nozzle toward the pad's surface. As the solder ball descends, it still maintains a spherical shape due to surface tension. Upon contact with the soldering pad, it spreads and wets the pad's surface, metallurgical reaction occurs, adhering effectively. When the solder ball reaches the surface of the pad, it remains in a molten state as a filler ball. Under the influence of surface tension, on one hand, the solder ball wets, spreads, and adheres to the pad surface; on the other hand, the solder ball will exhibit a certain degree of vibration. At the same time, within just a few milliseconds, the solder ball solidifies into a solder joint, signifying the end of the laser ball bonding process.

* Corresponding author. *E-mail address:* n.qian@nuaa.edu.cn(Ning QIAN)
Peer review under responsibility of Editorial Committee of JAMST
DOI: 10.51393/j.jamst.2025024

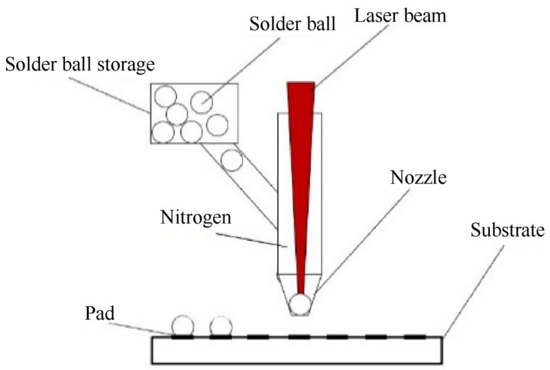

Fig. 1. Principle of LJSBB.

However, LJSBB encounters several challenges, including issues with reliability, precision in ball placement, energy dissipation, bridge connections, cracking, and tin splashes, among others [7]. To bolster the solder joint's reliability, extensive research indicates that elevating the laser power enhances the joint's shear strength and wettability, leading to a more comprehensive reaction with the solder pad. However too high or too low laser power will make the wettability worse, and it is easy to splash or even residual filler metal to the nozzle [8-10]. Yang et al. [11] employed finite element analysis to study the impact of laser power on the solder joint's temperature and thermal stress, which correlated with both power intensity and heating duration. The findings suggested that a judicious increase in laser power facilitates the development of a refined and uniform microstructure, thereby enhancing micro-hardness. Fu et al. [12] heated the bottom of the device when planting balls to improve the reliability of the solder joints. Aiming to enhance the accuracy of ball placement, Chen[13] introduced an innovative algorithm for laser temperature control, thereby refining the precision of the soldering process. Li et al. [14] leveraged a residual neural network for the prediction of process parameters, demonstrating minimal overshoot and swift dynamic response capabilities. To improve the energy utilization rate of laser ball planting, Tatsumi et al. [15] engineered an innovative device that employed a blue diode laser instead of the conventional infrared laser. This cutting-edge technology boasts a superior metal absorption rate, translating to greater efficiency and energy conservation.

Despite these advancements, the current body of research is sparse regarding the specific impact of Laser Jet Solder Ball Bonding process parameters on the geometry of solder joints and the resultant coplanarity, as illustrated in Fig. 2. Solder joint coplanarity refers to the flatness of the solder joints surface on the same level plane, that is, the maximum height difference between the top surfaces of all solder joints relative to each other. Typically, the plane formed by the three highest points is chosen as the reference plane, and the distance from the lowest solder joint to the reference plane is the coplanarity. Suboptimal coplanarity can precipitate the occurrence of virtual soldering during the subsequent reflow soldering, a phenomenon that not only compromises the product's reliability but also diminishes manufacturing productivity. Addressing these gaps in knowledge is essential for refining the LJSBB process and ensuring the delivery of electronic components.

On the other hand, shearing force and interface microstructure (especially the intermetallic com-pounds) are important criteria for the reliability of solder joints. The continuity and thickness of intermetallic compounds in the interface microstructure mainly determine the shearing force of the solder joints. Zhang[16] found that

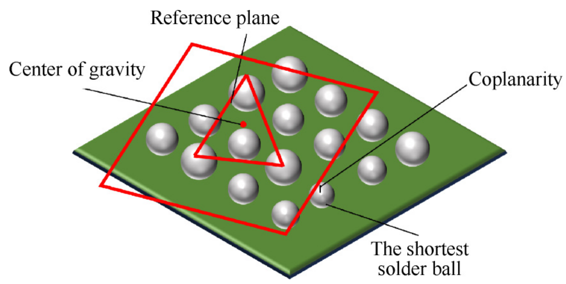

Fig. 2. Coplanarity of solder joints.

when optimizing parameters, the laser height should be slightly above the position of the solder pad to obtain a wider process window, and then appropriately adjust the laser power and time to achieve better and more stable laser ball bonding strength. Yang et al. [17] observed the interface micro-structure of manual soldering and LJSBB solder joints by comparison and found that the intermetallic compounds were more continuous and uniform. Wang[18] conducted LJSBB on thick gold pads and found that due to the limited heat, the gold layer could not be completely dissolved into the solder, resulting in the formation of multiphase compounds at the interface. However, there is currently a lack of research combining the shearing force of solder joints with their interface microstructure, as well as studies on how laser process parameters affect the interface microstructure and intermetallic compounds of solder joints, thereby influencing their shearing force.

The rapid heating and cooling dynamics inherent to laser ball planting technology significantly influence the shape, coplanarity, and shearing force of the solder joints. Despite the importance of these factors, there is a dearth of research dedicated to the coplanarity of joints formed by Laser Jet Solder Ball Bonding. This paper addressed this gap by focusing on Sn63Pb37 solder balls, 500 μm in diameter, bonded onto PCB substrates was pads Au/Ni/Cu as the subjects of this institute. Through some meticulous single factor experiments, the paper dissected the impact of each process parameter on the shape, coplanarity, shearing force, and solder joint interface microstructure. Employing the response surface methodology, this institute further explored the interplay between the various process parameters about how to influence the coplanarity and shearing force. The aim was to meticulously tune these parameters to optimize the coplanarity and shearing force of the solder joints, ensuring a higher standard of joint uniformity and quality over the GJB 7677. By leveraging this comprehensive approach, the research endeavors to enhance the precision and reliability of Laser Jet Solder Ball Bonding processes, contributing valuable insights to the field of electronic packaging.

2. Experiment condition

2.1. Test materials and instruments

In this experimental investigation, Sn63Pb37 solder balls, each with a precise diameter of 500 μm, were utilized in conjunction with PCB substrates. The substrates were dimensioned at 10 mm by 10 mm by 1 mm, featuring solder pads with a diameter of 450 μm. These pads were meticulously plated with a layer of nickel followed by a final layer of gold to ensure optimal bonding conditions.

The experimental setup included an automatic tin ball soldering machine, ABT-200D from Anewbest Company, which is a sophisticated assembly integrating an automatic control system, laser module, nitrogen supply system, mobile platform, and a camera system as depicted in Fig. 3. The laser operates as a wavelength of 1064 nm with a maximum power output of 150 W. In the context of this study, laser power was expressed as a percentage of the total power, with 10% equating to 15 W.

The operational mechanism of the equipment involves capturing an image of the soldering pad on the components and defining the soldering trajectory and process parameters. Subsequently, the motion control system maneuvers the nozzle above the pad. The ball system then delivers the tin ball to the nozzle, where the laser beam liquefies it. The molten ball is propelled towards the pad by the nitrogen, forming a bond. The coplanarity of the solder joints is ascertained through 3D scanning technology using a 3D profiling instrument, VR5000, which measures the maximum deviation to determine the coplanarity of the joints. This methodological approach ensures a thorough assessment of joint uniformity and quality. The shearing force is measured using a shearing force tester, BS5KG, with a cutting tool having a width of 700 μm.

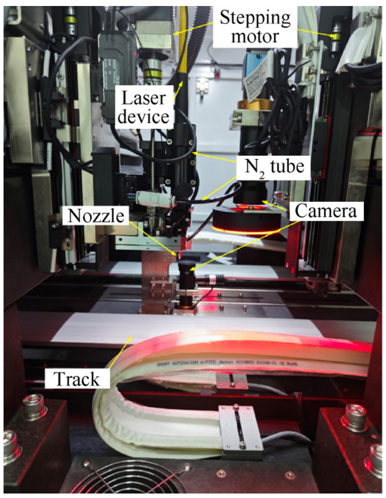

Fig. 3. LJSBB device and its composition.

2.2. Single factor experiment design

To explore the influence of process parameters on the shape and coplanarity, the influence of the main parameters of laser power, heating time, and nozzle height on the shape, coplanarity (G), and shearing force (F) was shown through the control variable method. Based on the suggestions provided by Anewbest, this paper selects the following parameters for the experiment. Each single factor parameter was laser power (W), heating time (T), and nozzle height (H). The first experiment process parameters were laser power 37%-45%, heating time 7 ms, and nozzle height 0.6 mm. The second was laser power 38%, heating time 7-11 ms, nozzle height 0.6 mm. The last experiment process parameters were laser power 38%, heating time 8 ms, and nozzle height 0.6-0.8 mm. This experiment aims to investigate the influence of process parameters on the performance of solder joints, in preparation for subsequent process optimization. The selected variable and non-variable parameters will have no impact on the subsequent optimization process.

3. Experiment result and analysis

3.1. Result of single factor experiment

The experiment results revealed that an escalation in laser power led to a transformation in the solder joint's morphology. Initially, the joints presented a more uniform spherical shape, but as power increased, they evolved into irregular surfaces characterized by pits and even flattened out. Concurrently, the coplanarity of the solder joint experienced an initial decline followed by an increase, as shown in Figs.4(a) and 4(d).

What's more, the results demonstrated that as the heating time was increased, the solder joints, while initially spherical, gradually developed flat areas. A rising incidence of flat solder joints was observed, correlating with a consistent decline in joint coplanarity. It was evident upon close observation that an extended heating duration significantly amplifies the prevalence of flat solder joints, culminating in reduced coplanarity, which was gleaned from Figs.4(b)

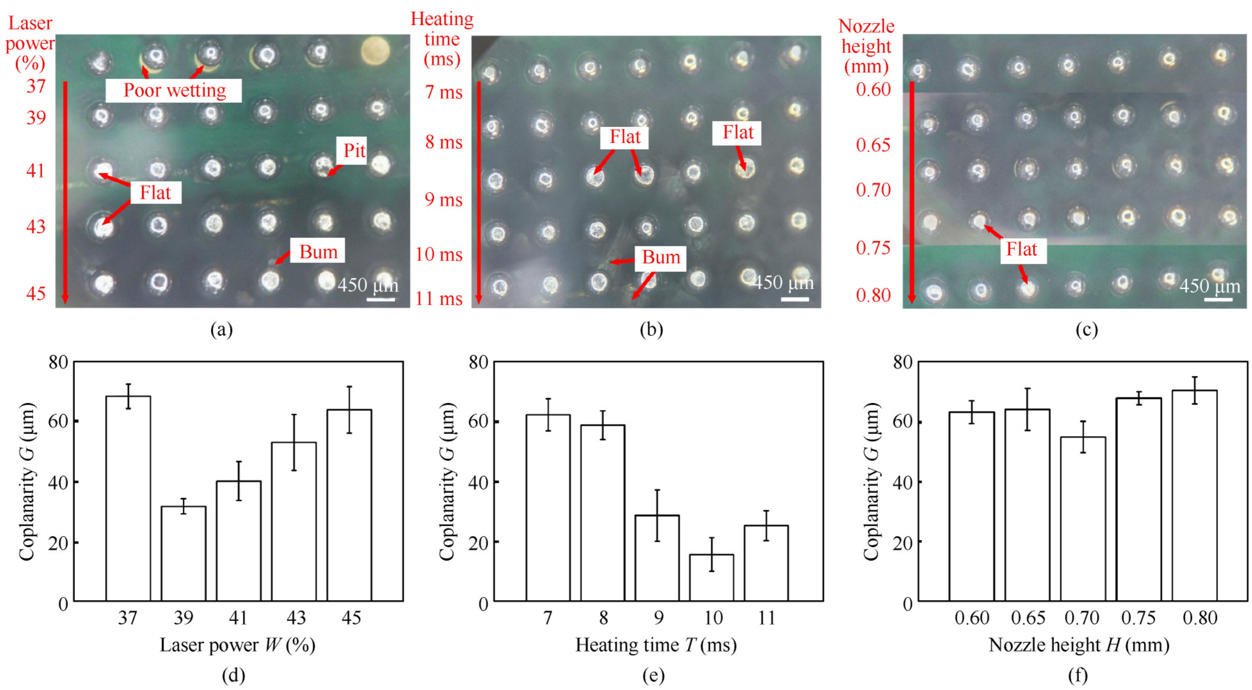

Fig. 4. Influence on shape and coplanarity: (a) Power on shape, (b) Heating time on shape, (c) Nozzle height on shape, (d) Power on coplanarity, (e) Heating time on coplanarity, (f) Nozzle height on coplanarity.

and 4(e). At last, the results illustrated the impact of nozzle height on solder joint shape and coplanarity. Within the nozzle height range of 0.6 to 0.7 mm, the solder joint shape remains relatively consistent. However, as the nozzle height extended beyond this range, the emergence of flat solder joints became more pronounced. The coplanarity of the solder joints declined within the 0.6-0.7 mm height range and then reversed, showing an increase when the nozzle height spaned from 0.5 to 0.8 mm, which was shown in Figs.4(c) and 4(f).

Through the results, it was clear that process parameters influenced the shape of solder joints, and the different shapes between solder joints using the same process parameters made solder joints coplanarity change. It was also clear that changing heating time made the shape of solder joints change the most so the coplanarity was changed the most as well. This visual analysis underscored the intricate relationship between process parameters and the physical attributes of solder joints, highlighting the necessity for precise control over these variables to ensure optimal joint formation and coplanarity.

The experimental results revealed the significant impact of laser power and heating time on the shearing force of the solder joint. Specifically, with the nozzle height fixed at 0.6 mm and a heating time of 7 ms, the shearing force of the solder joint showed a clear upward trend as the laser power increased, a trend demonstrated in Fig. 5 (a). This indicates that under lower heating times, increasing the laser power can effectively promote the melting and flow of the solder, thereby enhancing the bonding strength of the solder joint. Further experiments observed that when the laser power was set to 38%, with the nozzle height also maintained at 0.6 mm, the shearing force of the solder joint increased significantly with the extension of heating time, as shown in Fig.5 (b). This suggests that under the action of higher laser power, extending the heating time can provide more energy to the solder, allowing it to more fully wet the pad and form a more robust solder joint. Soldered joints under these conditions exhibit higher shearing forces, reflecting their superior mechanical properties and reliability. In contrast, adjusting the nozzle height had a less significant impact on the shearing force of the solder joint (as shown in Fig. 5 (c)).

3.2. Analysis and discussion

The experimental findings elucidated a strong correlation between the coplanarity and the shape of the solder joints. The shape of the joint was intricately linked to the trajectory of the molten tin ball as it landed on the pad's surface, the subsequent solidification phase, and the interplay of physical properties such as surface tension and viscosity. Notably, laser power and heating time exert substantial influence on the joint's configuration. An increase in either power or duration resulted in a pronounced transition from a spherical to a flatter form, with coplanarity adjusting in tandem. The formation of the molten solder joint adhered to the principle of energy minimization. Upon reaching a state of static equilibrium, the energy within the three-phase system of the solder joint, comprising the liquid phase and the solid and gas phases in contact with it, should be at its lowest [19]. This principle dictated that the solder joint naturally sought the configuration that minimizes its surface energy, leading to the observed morphological changes in response to variations in laser power and heating time. This understanding of the underlying physical phenomena provided a foundation for optimizing the soldering process, ensuring that joints achieved the desired shape and coplanarity, which were paramount for the structural integrity and performance of the electronic assembly.

On one hand, an increase in laser energy elevated the temperature of the molten filler metal, subsequently impacting its density and surface tension, as delineated by Eqs. (1) and (2). This alteration also influenced the wetting angle and the maximum spreading diameter of the soldering ball [20]. As per Eq. (3), these changes resulted in a modification of the surface energy (E_s), making it increasingly challenging to preserve the spherical form of the ball upon impact with the pad. Consequently, the molten ball's ability to maintain its shape was compromised, leading to variations in the solder joint's geometry post-solidification.

$$\sigma(T) = \sigma_0 - \frac{d\sigma}{dt} T \quad (1)$$

$$\rho(T) = \rho_0 - \frac{d\rho}{dt} T \quad (2)$$

$$E_s = \iint_A \sigma \, dA \quad (3)$$

On the other hand, when the laser irradiated the surface of the soldering balls, a localized increase in temperature was observed, creating a melt pool with a higher temperature than the surrounding areas. Under the laser's influence, substantial metal vapor and photo plasma were produced. The recoil from these phenomena forced the molten pool, deforming it and often causing the formation of a small hole [21]. As laser power and heating time increased, so too did the temperature of the molten pool. Upon ejection from the nozzle, the molten ball experienced a more pronounced force due to the nitrogen, leading to a flatter contact surface when it reached the pad, resulting in a flattened solder joint shape. The duration of heating significantly influenced the solder joint shape; an extended heating time increased the laser energy absorbed by the soldering ball [22,] enhancing the fluidity of the solder and leading to a higher incidence of flat solder joints compared to standard joints. This was a key factor contributing to the reduction in joint coplanarity.

Nozzle height predominantly affected the kinetic energy of the ball just before it struck the pad. Eq. (4) represented an energy conservation model, postulating that the energy before and after the

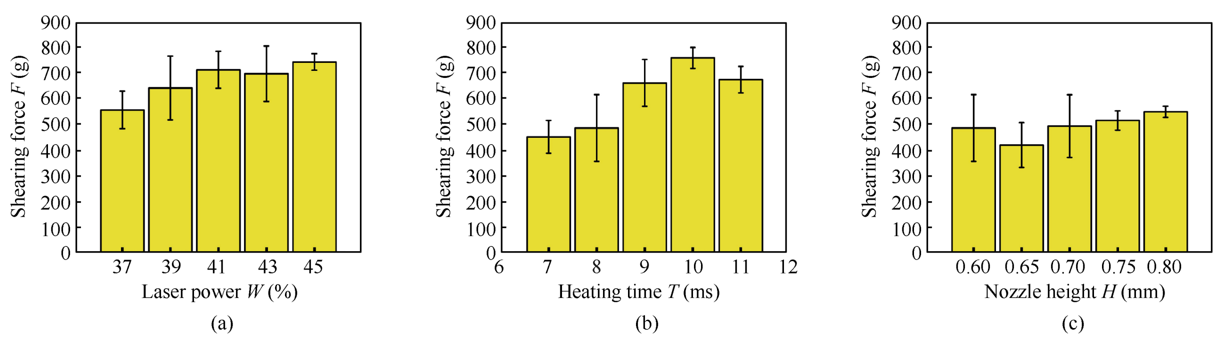

Fig. 5. Influence on shearing force: (a) Power on shearing force, (b) Heating time on shearing force, (c) Nozzle height on shearing force.

droplet's impact was equivalent to the energy at the point of maximum spreading diameter[23]. This indicated that kinetic energy (E_k) rose with nozzle height, while surface energy variations were minimal. The combined effect of the energy changed during spreading (E_p) and the viscous energy dissipation (W_s) increased. As previously outlined, the increased kinetic energy upon ball ejection accelerated penetration of the pad surface, and the reaction force amplified the oscillation amplitude of the soldering ball. Given manufacturing tolerances, each ball's oscillation amplitude varied, and these variations were exacerbated as the amplitude increased, leading to differing changes in E_p and W_s. According to Eq. (5), the height of the solder joint (h) adjusted accordingly, impacting the joint's shape during solidification and, by extension, its coplanarity to a noticeable degree, but the characteristic time of viscous energy dissipation (t_c) nearly never changed.

$$E_k + E_1 = E_2 + E_p + W_s \tag{4}$$

$$W_s \approx \mu^{(\frac{U0}{h})^2 V} t_c \tag{5}$$

It could be seen from the above analysis that the laser power and heating time directly affected the shape changes of the soldering ball by affecting the surface tension of the solder ball and the temperature of the molten pool. The nozzle height affects the solder joint shape mainly by altering the kinetic energy of the solder ball when it contacts the pad surface, which in turn influences the amplitude of the solder ball's vibration after wetting the pad surface, affecting the morphological differences as the solder ball solidifies into a solder joint, and thus can affect the coplanarity of the solder joint to a certain extent.

The shearing force of a solder joint is significantly influenced by the intermetallic compound (IMC) layer within the joint's interfacial microstructure. The continuity and thickness of the IMC layer are decisive factors for the shearing force of the solder joint. Generally, the thinner, denser, and more uniformly distributed the IMC layer is, the better the shear performance of the solder joint. This is because a thinner IMC layer helps to reduce stress concentration within the joint, thereby enhancing the mechanical strength and reliability of the solder joint.

When Sn63Pb37 reacted metallurgically with the gold-plated layer on the pad surface, brittle Au-Sn phases were formed. The experiment above uses some same parameters to show the influence of the interfacial microstructure. As the metallurgical reaction between the solder and the pad progresses, the content of Au-Sn phases increases, which can easily reduce the shearing force of the solder joint and make it more prone to brittle fracture. To simplify the experimental process, this study only selected three different points of laser power and heating time to observe the interfacial microstructure.

By observing the effect of laser jet solder ball bonding process parameters on the morphology of the IMC layer in the solder joint, we found that as the laser power or heating time increases, the IMC layer transitions from a dispersed discontinuous state (as shown in Figs. 6(a) and 6(b)) to a uniform and thinner layer (as shown in Figs. 6(c) and 6(d)). If the laser power or heating time is further increased, the average thickness of the IMC does not change significantly, but a coarser IMC morphology may appear as shown in Figs. 6(e) and 6(f). This indicates that an increase in laser energy can make the IMC layer rougher, which may not affect the shearing force of the solder joint but can increase its brittleness. On the other hand, in subsequent applications such as reflow soldering, larger Au-Sn IMC phases may grow further, increasing in thickness, which will significantly reduce the shearing force.

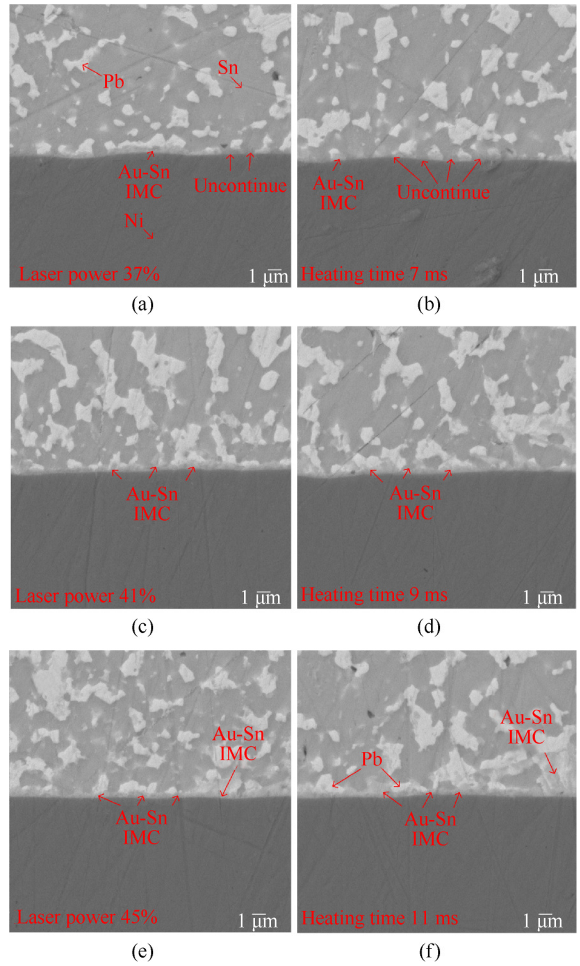

Fig. 6. Microstructure at the solder joint interface varies with laser power and heating time: (a) Laser power at 37%, (b) Heating time of 7 ms, (c) Laser power at 41%, (d) Heating time of 9 ms, (e) Laser power at 41%, (f) Heating time of 11 ms.

4. Process optimization and analysis

4.1. Response surface experiment design

To optimize the process parameters and analyze the interaction effect of each parameter on the coplanarity of the solder joints, the response surface method (Box-Benhnken, BBD) was used to carry out the experiment, which has the characteristics of short period and high precision. Assuming that there were n measurable and controllable independent variables, the functional relationship between them and the response value was generally expressed by quadratic polynomial, and the equation as

$$R = \gamma_0 + \sum_{i=1}^{n} \gamma_i x_i + \sum_{j=1}^{n} \gamma_j x_j^2 + \sum_{k=1}^{n} \sum_{l=1}^{n} \gamma_{kl} x_k x_l + \varepsilon \tag{6}$$

where R was the predicted response value; γ was the regression coefficient; and ε was the error term.

To delve into the collective impact of diverse process parameters on the coplanarity of solder joints, laser power, heating time, and nozzle height as the key factors for response surface analysis. By examining the data presented in Fig. 4, aiming to preserve the rounded shape of the solder joints and minimize the occurrence of flat joints, which were less desirable.

With this objective in mind, the experimental levels for these parameters were carefully chosen and are detailed in Table 1. This strategic selection ensured a comprehensive evaluation of how these variables interacted and their cumulative effect on achieving optimal coplanarity, thereby enhancing the quality and reliability of the solder joints.

Table 1 Experiment factors and levels.

Factor	*W* (%)	*T* (ms)	*H* (mm)
Level 1	38	7	0.6
Level 2	39	8	0.65
Level 3	40	9	0.7

4.2. Response surface experiment scheme and results and analysis of model variance

Taking the coplanarity and shearing force of solder joints as the response value, 17 groups were designed. The design scheme and results are shown in Table 2.

Table 2 Result of response surface experiment.

No.	*W* (%)	*T* (ms)	*H* (mm)	*G* (μm)	*F* (g)
1	39	7	0.6	44.69	566.992
2	38	8	0.6	65.63	411.336
3	39	7	0.7	41.37	510.908
4	39	8	0.65	57.44	576.628
5	39	9	0.6	19.01	562.984
6	39	9	0.7	12.88	733.336
7	39	8	0.65	54.52	642.12
8	40	8	0.7	53.02	641.556
9	38	7	0.65	68.38	386.676
10	38	9	0.65	20.39	602.172
11	40	8	0.6	48.23	584.316
12	40	9	0.65	33.46	650.504
13	40	7	0.65	51.71	668.58
14	38	8	0.7	51.57	523.712
15	39	8	0.65	57.16	658.432
16	39	8	0.65	60.28	626.812
17	39	8	0.65	57.39	607.576

The predictive model for the impact of LJSBB process parameters on solder joint coplanarity and shearing force, obtained through Design Expert software, are as Eqs. (7) and (8).

By analyzing the data of the two models through Tables 3 and 4, it could be observed that both models showed significant results, and the lack of fit for both were not significant, proving their high reliability. Additionally, through Table 5, the R^2 values for both models are greater than 0.85, and the difference between R^2_{Pred} and R^2_{Adj} is less than 0.2. It proved that these models could be used to predict the coplanarity and shearing force of solder joints for the material combination and specifications in question.

$$G = 56.86 - 2.43W - 13.92T - 1.92H + 7.89WT + 4.36WH - 2.8TH + 6.88W^2 - 19.73T^2 - 8.3H^2 \quad (7)$$

$$F = 662.31 + 77.63W - 51.98T - 35.49H - 58.39WT - 13.78WH + 56.61TH - 49.33W^2 + 4T^2 - 32.76H^2 \quad (8)$$

4.3. Influence of process parameters on coplanarity and shearing force of solder joints

The response surface methodology provided a visual and intuitive representation of how two variables simultaneously affected a dependent variable. The steepness of the response surface was indicative of the magnitude of impact; a steeper slope suggested a more pronounced effect. The contour map of the response surface was assessed for its roundness, with more elliptical contours signifying a more substantial interaction between the two independent variables.

Utilizing the Design Expert software, it constructed interactive response surface diagrams that illustrated the combined effects of laser power, heating time, and nozzle height on the coplanarity of solder joints from the aforementioned experiments.

According to the software analysis results, it was known the influence of laser power and heating time on solder joint coplanarity. Its diagram indicated a steep response surface within the 8.5-9 ms

Table 3 Analysis of coplanarity model.

Source	Sum of square	df	Mean square	F	P
model	6233.74	9	692.64	88.89	< 0.0001
W	88.44	1	88.44	11.35	0.0036
T	2092.10	1	2092.10	268.48	< 0.0001
H	49.09	1	49.09	6.30	0.0225
WT	463.91	1	463.91	59.53	< 0.0001
WH	176.25	1	176.25	22.62	0.0002
TH	49.96	1	49.96	6.41	0.0215
W^2	278.60	1	278.60	35.75	< 0.0001
T^2	2408.76	1	2408.76	309.12	< 0.0001
H^2	394.61	1	394.61	50.64	< 0.0001
Residual	132.47	17	7.79		
Lack of fit	63.11	7	9.02	1.30	0.3413
Pure error	69.37	10	6.94		
Cor total	6366.21	26			

Table 4 Analysis of shearing force model.

Source	Sum of square	df	Mean square	F	P
model	1.226×10^5	9	13627.13	20.50	0.0003
W	48214.44	1	48214.44	72.52	< 0.0001
T	21615.36	1	21615.36	32.51	0.0007
H	10073.77	1	10073.77	15.15	0.0060
WT	13638.97	1	13638.97	20.52	0.0027
WH	759.99	1	759.99	1.14	0.3205
TH	12818.32	1	12818.32	19.28	0.0032
W^2	10245.19	1	10245.19	15.41	0.0057
T^2	67.27	1	67.27	0.10	0.7597
H^2	4517.65	1	4517.65	6.80	0.0351
Residual	4653.65	7	664.81		
Lack of fit	632.21	3	210.74	0.21	0.8850
Pure error	4021.44	4	1005.36		
Cor total	1.273×10^5	16			

Table 5 Analysis of models.

Model	R^2	R^2_{Pred}	R^2_{Adj}
G	0.9792	0.9305	0.9682
F	0.9634	0.8712	0.9164

range, highlighting a significant interaction between these two factors (Figs. 7 (a) and 7(d)). As laser power increased, the coplanarity of the solder joint initially decreased and then subsequently increased. However, within the 7-8.5 ms interval, the interaction effect between laser power and heating time was observed to be negligible.

The laser power and nozzle height on the coplanarity of solder joints showed their interactive effects as well. Its diagram and response surface analysis revealed that within the laser power range of 38%-39% (Figs. 7(b) and 7(e)), an increase in nozzle height resulted in a deceleration of the decrease in coplanarity, suggesting a stabilizing effect on joint flatness. However, when laser power was adjusted to the 39%-40% range, the interaction with nozzle height became negligible, indicating that the nozzle height's impact on coplanarity was less pronounced at higher power levels.

Heating time and nozzle height on solder joint coplanarity also presented the interactive effects. A detailed examination of the response surface and its corresponding contour map revealed that within a heating period of 8-9 milliseconds, the response surface exhibited a steep gradient (Figs. 7(c) and 7(f)). This indicated a significant interplay between heating time and nozzle height. As nozzle height increased, the rate at which joint coplanarity diminishes initially became more rapid, followed by deceleration, suggesting a complex dynamic between these variables.

In contrast, when the heating time is confined to the 7-8 millisecond interval, the interaction effect between nozzle height and heating time was observed to be inconsequential.

According to the software analysis results, it was known the influence of laser power and heating time on solder joint coplanarity. Through the response surface plots in Figs. 8(a) and 8(d), it can be observed that within the range of 38% to 39% laser power, there is an interactive effect between laser power and heating time on the shearing force of the solder joint. As the heating time increases, the increase in laser power accelerates the rate at which the shearing force of the solder joint rises. This is due to the increased laser energy, which provides more heat for the metallurgical reaction between the solder and the pad, making the reaction more complete and the IMC more uniform, hence the shearing force increases more rapidly until it reaches the maximum value within the specified parameters. The interactive effect between laser power and nozzle height is even more pronounced. As the laser power increases, raising the nozzle height first increases and then decreases the rate at which the shearing force of the solder joint rises. This indicates that the heat of the solder joint during the reaction with the pad is affected by the nozzle height, especially when the laser power varies (as shown in Figs. 8(b) and 8(e)). Heating time and nozzle height also have a certain interactive effect on the coplanarity of the solder joint. As the heating time increases, raising the nozzle height first decreases and then increases the rate at which the shearing force of the solder joint rises (as shown in Figs. 8(c) and 8(f)).

4.4. Optimization of process parameters

The Design Expert software was adeptly utilized to identify and refine the optimal combination of process parameters, targeting the minimization of solder joint coplanarity. The outcome of this optimization exercise is as detailed below: the laser power was set at 38.708%, the heating time at 9 ms, and the nozzle height at 0.7 mm. The software predicted a coplanarity of 12.880 μm, which was closely mirrored by the actual measured value of 12.917 μm, yield-

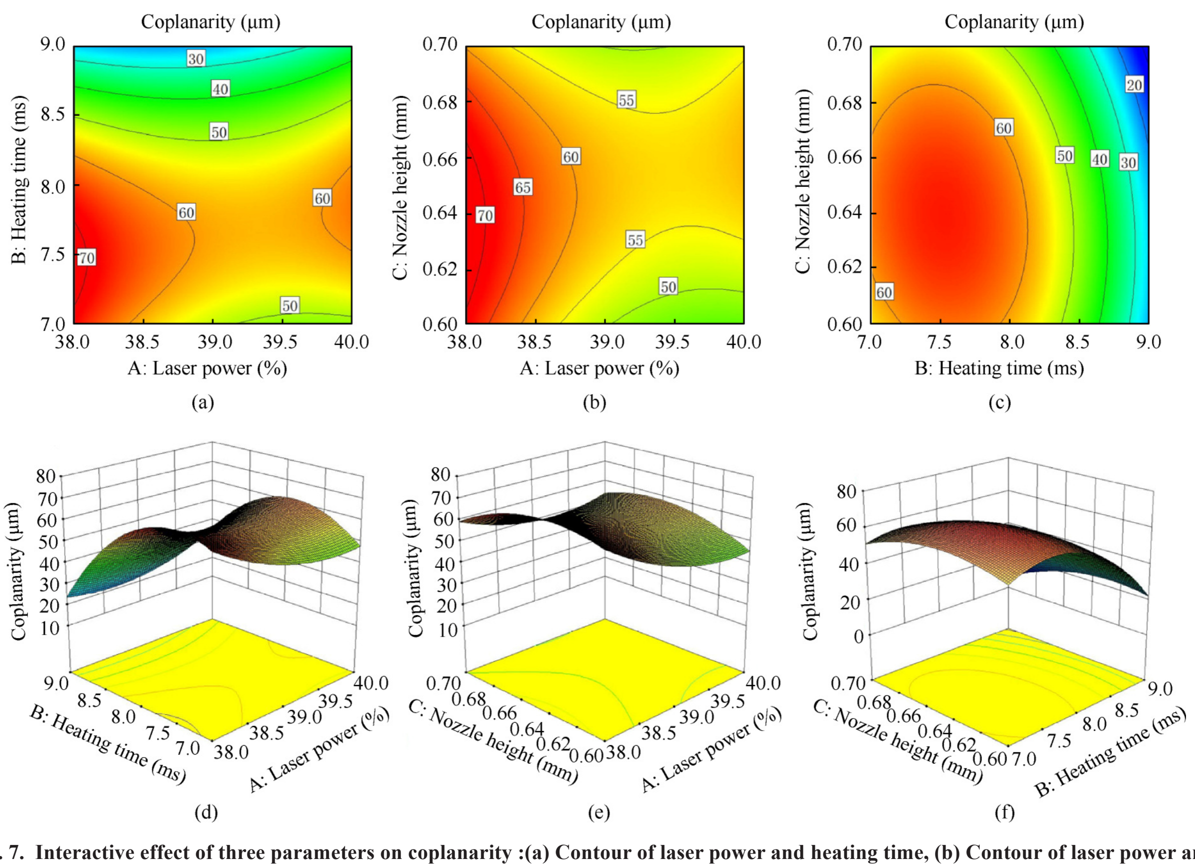

Fig. 7. Interactive effect of three parameters on coplanarity :(a) Contour of laser power and heating time, (b) Contour of laser power and nozzle height, (c) Contour of heating time and nozzle height, (d) 3D surface of laser power and heating time, (e) 3D surface laser power and nozzle height, (f) 3D surface of heating time and nozzle height.

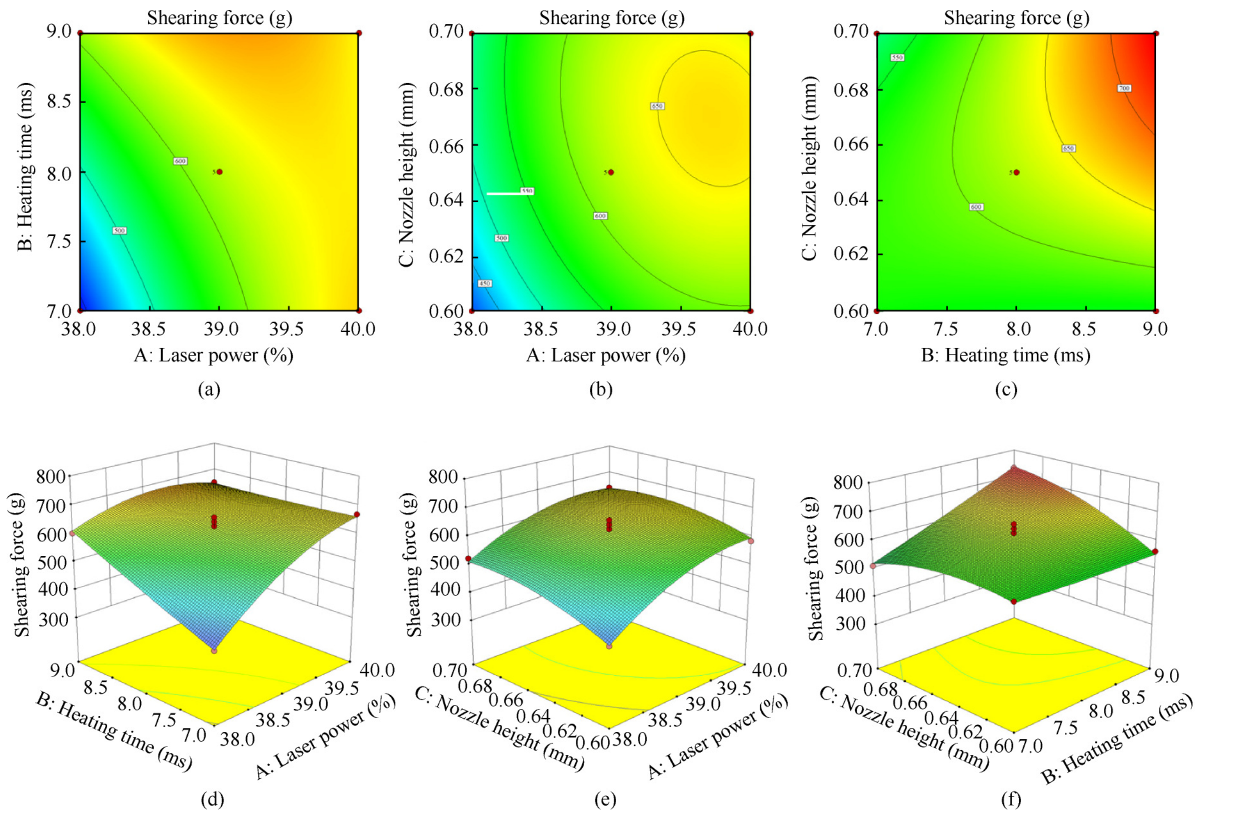

Fig. 8. Interactive effect of three parameters on shearing force :(a) Contour of laser power and heating time, (b) Contour of laser power and nozzle height, (c) Contour of heating time and nozzle height, (d) 3D surface of laser power and heating time, (e) 3D surface laser power and nozzle height, (f) 3D surface of heating time and nozzle height.

ing a prediction error of a mere 2.86%.

The shearing force is 731.836 g which was closely mirrored by the actual measured value of 702.473 g, yielding a prediction error of a mere 4.18%. The optimization results greatly met the coplanarity requirement (less than 0.15 mm) and shearing force requirement (more than 360 g) for the Sn63Pb37 solder joints of this size compared with GJB-7677. These results substantiated the reliability of the process parameters determined for the LJSBB technique, showcasing their efficacy in enhancing the coplanarity of solder joints.

5. Conclusion

This study delved into the influence of process parameters on the shape, coplanarity, and shearing force of solder joints. Experiments have revealed that laser energy affects the morphology of the solder joint by influencing the temperature of the solder ball melt pool, thereby affecting coplanarity. It also affects the continuity and thickness of the IMC layer by influencing the intensity of the metallurgical reaction between the solder ball material and the gold plating layer on the pad surface. Within a certain range, increasing laser energy can improve the coplanarity and shear strength of the solder joint. The nozzle height mainly affects the vibration of the solder ball after it contacts the pad, which in turn affects the solidified shape and thus the coplanarity of the solder joint, but has a smaller impact on the shear strength when the solder ball and PCB substrate are combined with this material.

Response surface experiments have shown that the three process parameters have certain interactive effects on both coplanarity and shear strength of the solder joint, providing ideas for further research related to process parameters. Through response surface optimization, solder joints with coplanarity and shear strength that far exceed the GJB-7677 standard were achieved. The outcome of this optimization exercise is as detailed below: the laser power was set at 38.708%, the heating time at 9 ms, and the nozzle height at 0.7 mm. The software predicted a coplanarity of 12.880 μm, which was closely mirrored by the actual measured value of 12.917 μm, yielding a prediction error of a mere 2.86%; the shearing force is 731.836 g which was closely mirrored by the actual measured value of 702.473 g, yielding a prediction error of a mere 4.18%.

These findings suggest that the response surface method is a valuable tool for optimizing solder joints and could serve as a reference for further research in the field of LJSBB.

Acknowledgments

This project was supported by the Fund of Prospective Layout of Scientific Research for Nanjing University of Aeronautics and Astronautics (No. 1005-ILB23025-1A), the Fund of Jiangsu Key Laboratory of Precision and Micro-Manufacturing Technology (No. 1005-ZAA20003-14), and Nanjing Institute of Electronic Equipment.

References

1. Xiong MY, Su HH, Zhao B, et al. Effects of Au/Ni coating thickness on enhancing the properties of InPb/MoCu solder joints in microwave modules. *Vacuum* 2023;210:111905.
2. Xiong MY, Zhang L. Interface reaction and intermetallic compound growth behavior of Sn-Ag-Cu lead-free solder joints on different substrates in electronic packaging. *Journal of Materials Science* 2019;54 (2):1741-1768.
3. Kolbasow A, Fettke M, Kubsch T, et al. Study of solder interconnect configurations and performance of vertical laser assisted assembled “3.5 D” packages. *IEEE 70th Electronic Components and Technology*

Conference (ECTC). 2020：1936-1942.

4. Ismail AA, Bakar MA, Jalar A, et al. Laser rework process for efficient lead-free solder joints Ball Grid Array (BGA) component rework. *IEEE Transactions on Components, Packaging and Manufacturing Technology* 2024;14(4):735-742.
5. Fettke M, Kubsch T, Bejugam V, et al. A study about facile interconnect formations involving SB2-JET solder ball stacking and colonnade patterning in hybrid package architectures. *IEEE In 2020 International Wafer Level Packaging Conference (IWLPC)*. 2020:1-8.
6. Liu L. Research on ball planting technology of BGA connector. *Mechanical and Electrical Information* 2023;(15):72-76[Chinese].
7. Hwang S J, Hwang S V, Jung JP. Laser micro soldering and soldering factors. *Journal of the Microelectronics and Packaging Society* 2020; 27(3):1-8.
8. Chen H, Liang J, Gao R, et al. Laser soldering of Sn-based solders with different melting points. *IEEE 2020 21st International Conference on Electronic Packaging Technology (ICEPT).* 2020:1-5.
9. Hlinka J, Fogarassy Z, Cziráki Á, et al. Wetting properties, recrystallization phenomena and interfacial reactions between laser treated Cu substrate and SAC305 solder. *Applied Surface Science* 2020; 501: 144127.
10. Held C, Quentin U, Heberle J, et al. Laser droplet brazing for the electrical contacting of composite materials with integrated active elements. *Physics Procedia* 2012;39:585-593.
11. Yang Z, Li L, Chen W, et al. Numerical and experimental study on laser soldering process of SnAgCu lead-free solder. *Materials Chemistry and Physics* 2021;273:125046.
12. Fu YF, Hou XZ, Xu XJ, et al. BGA infrared ball planting technology. *Electronic Process Technology* 2023; 44(3):55-59[Chinese].
13. Chen Z. Data-based thermodynamic model and feedforward-PI control method for laser soldering. *The International Journal of Advanced Manufacturing Technology* 2023;129(11):5249-5260.
14. Li M, Cao P, Zhang C, et al. Variable-structure proportional-integral-derivative laser solder joint temperature intelligent control method with adjustable power upper limit. *Micromachines* 2023;14(8):1618.
15. Tatsumi H, Kaneshita S, Kida Y, et al. Highly efficient soldering of Sn-Ag-Cu solder joints using blue laser. *Journal of Manufacturing Processes* 2022;82:700-707.
16. Zhang H. Effects of laser ball planting parameters on shear force of welded ball. *Electronics & Packaging* 2019;19(8):5-7[Chinese].
17. Yang ZJ, Li S, Li M, et al. Reliability analysis of solder joints obtained by laser jet solder ball bonding method. *Electronics Process Technology* 2023;44(01):26-29[Chinese].
18. Wang XL. Analysis of interface microstructure and reliability of laser jet solder ball bonding weld joints. *Acta Metallurgica Sinica* 2010;46 (9):1115-1120[Chinese].
19. Nigro NJ, Heinrich SM, Elkouh AF, et al. Finite element method for predicting equilibrium shapes of solder joints. *Journal of Electronic Packaging* 1993;115(2):141-146.
20. Wang D. Design and experimental study of laser fusion jet soldering system [dissertation]. Changchun: Jilin University, 2017[Chinese].
21. Wang N, Yan HY, Li H, et al. Research progress of wettability impact factors of cermets. *Special Casting and Non-Ferrous Alloys* 2019;39 (12):1315-1319[Chinese].
22. Ren TY. Analysis of Interaction between long pulse laser and metal. *Application of Optoelectronic Technology* 2011;26(6):28-32[Chinese].
23. Chandra S, Avedisian CT. On the collision of a droplet with a solid surface. *Proceedings: Mathematical and Physical Science* 1991;432:13-41.